JOURNAL OF MATERIALS SCIENCE: MATERIALS IN MEDICINE 5 (1994) 243–251

The early host and material response of hydroxyapatite/β-tricalciumphosphate porous ceramics after implantation into the femur of rats

ZHANG JIANGUO, ZHANG XINGDONG
Institute of Material Science and Technology, Sichuan University, Chengdu, Sichuan, Peoples Republic of China

C. MÜLLER-MAI, U. GROSS*
Department of Traumatology and Reconstructive Surgery and Institute of Pathology, Klinikum Steglitz, Freie Universität Berlin, Hindenburgdamm 30, D 12200 Berlin, Germany*

The early responses of host and hydroxyapatite/β-tricalciumphosphate (HA-TCP) porous ceramic implants were studied using light microscopy (LM), scanning electron microscopy (SEM), and transmission electron microscopy (TEM) at 3, 7, 14, 21, and 28 days after implantation into the femur of rats. Micropores (< 5 μm) and macropores of the implant surface provided effective structures for anchoring of various tissue components. Mineralization started directly on the implant surface and was observed in macropores and micropores, suggesting bone-bonding by epitaxis. Bone-bonding was observed with and without an amorphous intervening interface layer. The composition of this layer and the mechanisms guiding its production are not yet fully understood. Extracellular matrix filled up the clefts between HA-TCP crystal grain clusters. These processes contributed to the mechanical stabilization of the interface. Slight changes of implant grain surface morphology were observed which were explained by leaching of impurities, such as TCP and/or by dissolution acting on single grains. Diameters of pores and HA-TCP grains did not change in a period up to 28 days, which seems to be related to the relatively short periods of insertion and the material properties. Leaching and degradation were observed and loose particles of implant origin were phagocytosed by macrophages and multinuclear giant cells which dominated at non-bonding interfaces.

1. Introduction

Hydroxyapatite ceramics, as bone implants, have long been the subject of intensive investigation. Included were various preparation methods, many different implant properties and clinical applications, and related research concerning the interface and bonding mechanisms [1–4]. As a development of these investigations, some researchers believed in the superiority of HA porous ceramics, to some extent, to other implants *in vivo* because of their structural similarity to bone trabeculae [5, 6].

Previous studies divided biomaterials into different categories, such as a bone-bonding species and a non-bonding species, and HA ceramics were classified as the former [7–9]. However, even though much work has been done to the interface between implant and host, the bonding mechanisms are still not yet fully understood.

In recent publications, it was shown that bone-bonding implants bond to bone via different interface layers. In the case of glasses or glass-ceramics, Si-rich, Ca/P-rich and amorphous layers were described between the mineralized bone and the bulk material [10–11]. In the case of HA implants, interfaces with or without an amorphous intervening layer were described [12, 13]. Up to now, it is not yet clear which mechanisms guide the development of such layers *in vivo* on Ca/P ceramics.

Studies based on the sequence of events at the interface of bone-bonding and non-bonding glasses and glass-ceramics indicated that four overlapping phases could be distinguished after insertion of implants: blood clot formation, formation of organization tissue, formation of primary bone and calcification which means regeneration of organ-typic tissue, and remodelling which lasts from months to years [14]. This view has been developed and more steps suggested in the development of bone and other tissue development at the interface of Bioglass® [15]. Basically, these phases are similar around different types of bone-bonding materials with quantitative differences in the type of tissue contact related to

0957–4530

different material properties. Additionally, there seems to be a lack of information concerning the early healing phases after insertion of porous HA implants. Recently, there evolved a discussion on the development of an afibrillar zone at the interface of bone-bonding materials and the significance of this process for the quality of the material–tissue interface [10–13, 16, 17]. Therefore, it is necessary to evaluate the early host and implant response, whereby more information might be obtained for understanding bone-bonding mechanisms.

The purpose of the present study was to investigate the early host and material response post implantation, i.e. especially the morphology of the HA-TCP porous ceramic interface in a bony implantation bed with regard to the development of amorphous interlayers, the anchoring and the sequence of events during the development of the various tissue components at the implant surface, and to gain new information about the establishment of bonding between HA-TCP and bone.

2. Materials and Methods

Composite hydroxyapatite/β-tricalciumphosphate (HA-TCP) was synthesized in accordance with aqueous solution coprecipitation under controlled conditions and sintering as previously documented [18]. The porous ceramic contained HA and as a second calcium phase 30% β-TCP. The implants displayed grains of about 0.5 μm in diameter prior to implantation. Macropores and micropores were measured (Table I). The total internal pore volume was 39%. The mean surface roughness was 6.5 μm, the Ca/P-ratio 1.67 ± 0.05, and the crystallinity 87%. The material was sawn in rectangular blocks (1 × 1 × 6 mm) and sterilized by autoclaving.

The description of the animal experimentation is given in [14]. After 3, 7, 14, 21, and 28 days postoperatively, the animals were sacrificed and the implants were collected and prepared for scanning electron microscopy (SEM), transmission electron microscopy (TEM), light microscopy (LM), and histomorphometry. A total of 28 animals was used. Four were used for LM at 7, 14, 21, and 28 days postoperatively; six were used for each, SEM and TEM. Of these, four were examined at 3 days, and two at 7, 14, 21, and 28 days. Details on the SEM, TEM and LM examination have been previously published [12, 19]. The specimens were examined with a Philips EM 410 transmission electron microscope.

3. Results

3.1. Material's surface characteristics

Before implantation, the implant surface was rather rough (as seen in the SEM) and macropores with a diameter between 70 μm and 150 μm could be observed. There were three kinds of surface structures of the HA implants. The most common surface structure consisted of sintered HA grains (Fig. 1a). These individual grains, with a mean diameter of 0.51 μm (Table I) were fused together at the grain boundaries by sintering and each single grain showed a smooth surface morphology which was the most dense surface structure. This morphology was confirmed in the TEM sections of the outer surface of HA-TCP ceramic implants (inset, Fig. 1a). The second kind of surface structure was discovered by sawing during the preparation of the blocks and seemed to be a surface of macropores. Interconnecting micropores with a mean diameter of 0.38 μm (Table I) were found between the grains in the macropores (Fig. 1b). The third surface structure was found between the grains of the outer implant surface parts and on inner macropore surfaces. These structures were detected as single grains or grain clusters and possessed a microroughness (Fig. 2a, b).

TABLE I Pore and grain diameters (μm) of HA porous ceramics before insertion and 28 days after implantation, n = number of measured structures, n.d. = not determined

Day	Macropore diameter	Micropore diameter	n	Grain diameter	n
0	70–150	0.38	216	0.51	127
28	n.d.	0.36	194	0.50	113

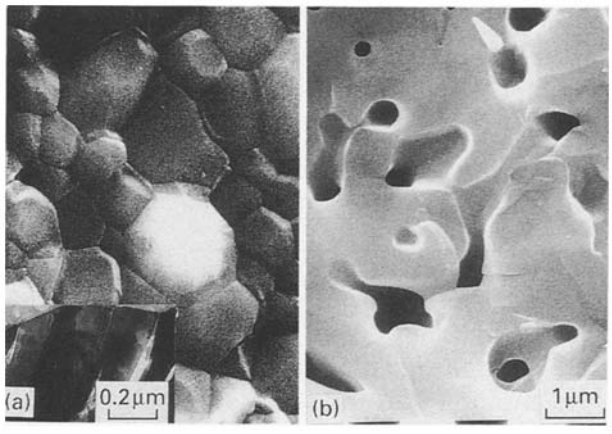

Figure 1 Implant surface structures prior to implantation with grains and pores. (a) Outer implant surface showing fused grains. (b) Inner pore surface discovered by sawing the implant blocks with dense fused HA-grains and micropores. Inset Fig. 1a: Outer implant surface of HA-TCP in the TEM with individual grains and smooth surface of grains.

3.2. Light microscopy and histomorphometry

At 7 days post-implantation, the space between the old bone surrounding the drill hole and the implant was partially filled by young bone trabeculae which were partially mineralized and located next to the old bone. Only a few connections of the new bone and the implant surface (2%) could be detected (Table II). Most of the implant surface was covered by soft tissue.

At 14 days postoperatively, the newly formed bone filled most of the space between implant surface and old bone of the drill hole. The bone connection areas increased to 27% (Table II). Osteoid and chondroid were not visible in the interface both at 7 and 14 days after implantation.

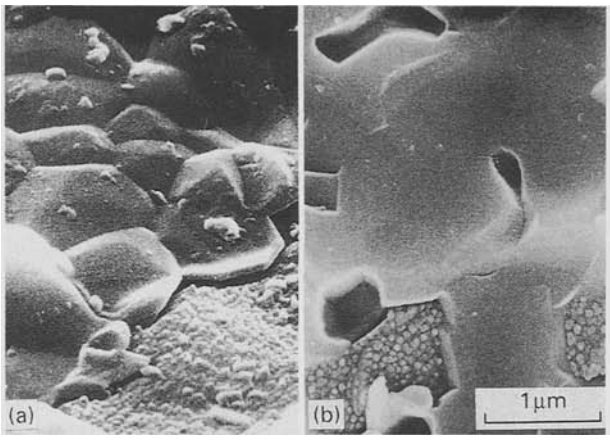

Figure 2 Implant surface structures with different morphology prior to implantation with grains and pores on outer implant surface (a) and on inner pore surface (b) as discovered by the sawing process. Rougher areas might correspond to TCP-content.

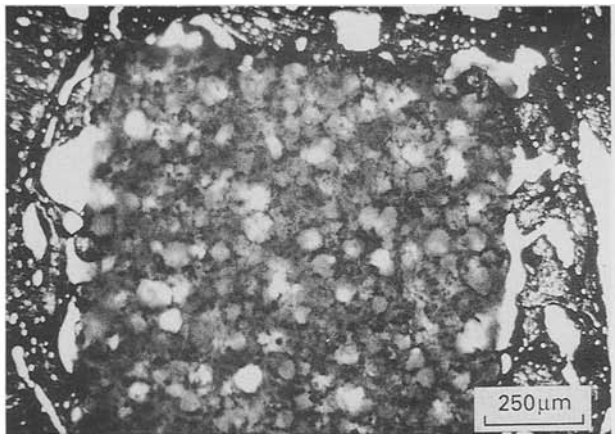

Figure 3 Cross-section of a HA-TCP implant at 28 days after implantation into the femur of a rat with dense old bone and younger trabecular bone filling most parts of the drill hole. Note porosity of the implant. LM, von Kossa stain.

TABLE II Percentage of bone, osteoid, and soft tissues in contact with the implant surface from 7 to 28 days after implantation, n = number of implants

Day	n	Bone	Osteoid	Soft tissue
7	4	2.14	0	97.86
14	4	27.28	0	72.72
21	4	49.83	0.40	49.77
28	4	68	0.41	31.59

At 21 and 28 days after implantation, the newly formed bone filled most of the drill hole and contacted areas of the implant to a greater extent than before (Table II) (Fig. 3). Osteoid (0.4%), but no chondroid could be detected in the interface, indicating that the mineralization was not disturbed at the implant surface. Young bone trabeculae developed in macropores of the implant surface. In all of the sawn sections, cells such as erythrocytes at 7 days, macrophages (Fig. 4a), osteoblasts, occasional multinuclear giant cells (Fig. 4b), and extracellular matrix (ECM) could be seen within macropores of the implant. The clefts among HA crystal grain clusters were also filled with ECM.

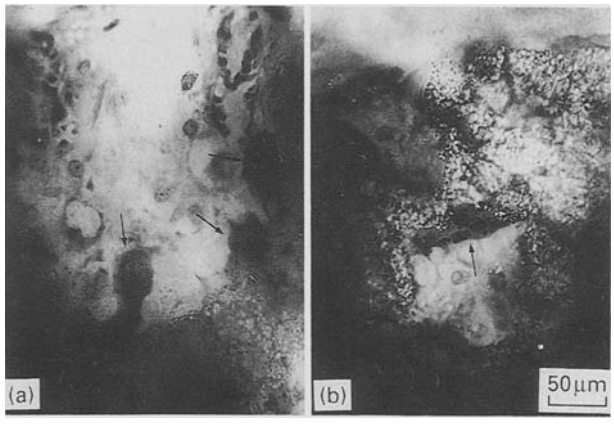

Figure 4 Cross-section of a HA-TCP implant at 28 days after implantation into the femur of a rat. (a) Macrophage-like cells in a pore in contact to the HA (arrows). (b) Multinucleated cell in contact to the inner pore surface (arrow). LM, Giemsa stain.

3.3. Scanning electron microscopy

At 3 days after implantation, the implant surface was mainly covered by remnants of the blood clot, including erythrocytes, many fibrillar structures and round cells. Fine fibrillar structures adhered to the implant surface and were also found within macropores. The surface of the implant material showed the same aspects as described before implantation, including different kinds of pores, grains, and areas which showed saw marks. Some single implant surface areas showed a fine granular material covering the grains which might be due to crystallization of inorganic material on the implant surface (Fig. 5).

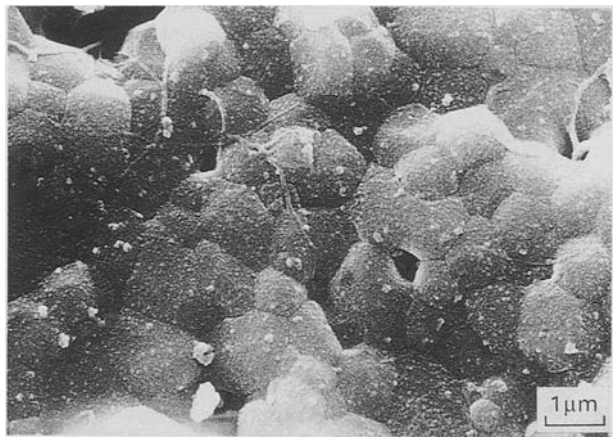

Figure 5 Outer implant surface structures at 3 days after implantation with grains and pores. Granular appearance probably due to crystallization at the implant surface; organic fibrillar remnants on the implant.

At 7 days, the exposed surface displayed remnants of tissue. The tissue consisted of a dense fibrous extracellular matrix (ECM) (Fig. 6) with many cells between. Most of the cells were roundish with many lamellopodia, located directly at the implant surface, and being considered as macrophases. Some spindle-

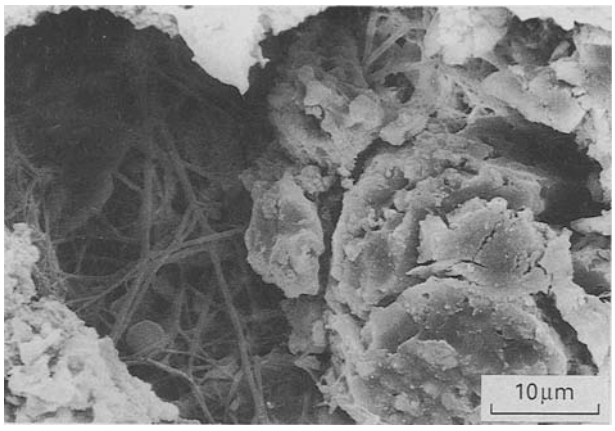

Figure 6 Outer implant surface structures at 7 days after implantation with a macropore (left), grains and micropores. Dense fibrillar network fills the macropore.

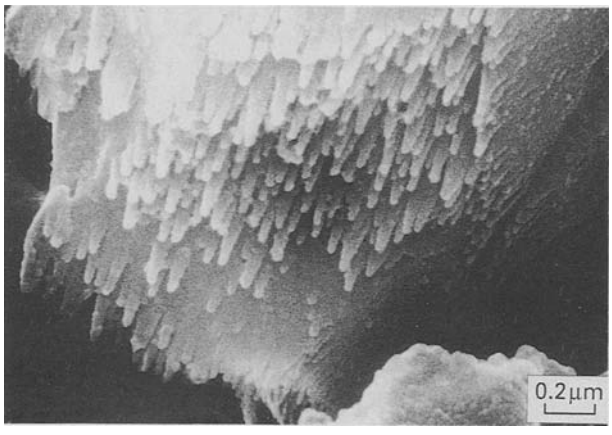

Figure 7 Outer implant surface grain at 14 days with needle-like tips on its surface of less than 0.1 µm in diameter.

like or polygonal cells were considered to be of osteoblastic type. The material surface showed the same aspect as described before. In a few areas, the smooth surface of single grains disappeared. Instead, a microroughness with tiny needle-like structures was seen which might have been induced by leaching or reprecipitation.

At 14 days after implantation, remnants of tissue, i.e. fragments of cells and ECM, covered most of the surface. Some larger trabeculae-like tissue fragments were seen. Fibroblastic, osteoblast-like cells and organic material appeared on the surface. In between this tissue, larger cells of about 15 µm in diameter were found which were similar to the macrophage-like cells at 7 days. A few giant cells of about 50 µm and more in length were discovered on the material surface. Locally leached areas of the material's surface could be observed. HA grains in these areas showed a rough surface with many needle-like tips with a diameter of about 0.1 µm (Fig. 7).

At 21 and 28 days after implantation remnants of tissue were also seen at the implant surface. Many areas with networks of fibres, probably collagen, interdigitated with the implant surface structures. Only few macrophage-like cells were detected, some of them showing filopodia being in close contact to roughened grain surfaces (Fig. 8). Saw marks were very seldom observed at 28 days. More leached areas with the typical roughness of the grains could be detected at the implant surface at 21 and 28 days after implantation. At 28 days after implantation, the mean diameters of both crystal grains and micropores had not changed when compared with those before implantation (0.50 µm and 0.36 µm, respectively) (Table I).

3.4. Transmission electron microscopy

At 3 days after implantation, the implant was covered with remnants of the blood clot, comprising electron dense fibrous fibrin-like material, erythrocytes, macrophages and some round cells (Fig. 9). The fibrin-like material was arranged in layers parallel to the implant surface or was in contact with the implant protruding into the macropores (Fig. 10). Fibroblast-like and osteoblast-like cells, recognized by the considerable amount of widened endoplasmic reticulum within the

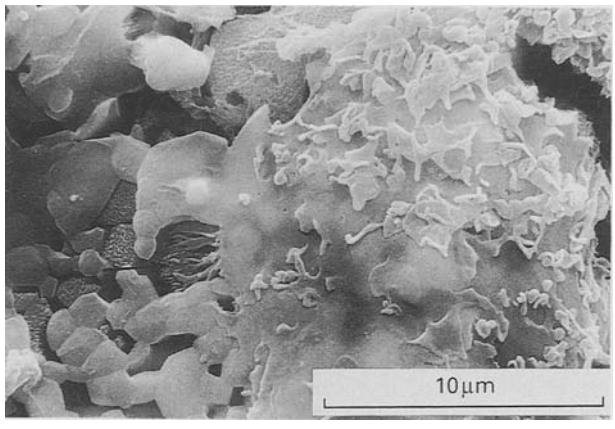

Figure 8 Outer implant surface at 21 days after implantation with grains and pores. Some grains with needle-like tips as described in Fig. 7. Part of a macrophage-like appearing cell with filopodia on its outer cellular membrane. Some filopodia in contact with roughened grain surface (arrow).

Figure 9 Outer implant surface at 3 days after implantation with HA-grains. Macrophage-like (M) cell in contact with the implant surface. Erythrocytes, polymorphnuclear leukocytes, already productive cells, and a cell containing phagocytosed implant material (I) in the implant vicinity.

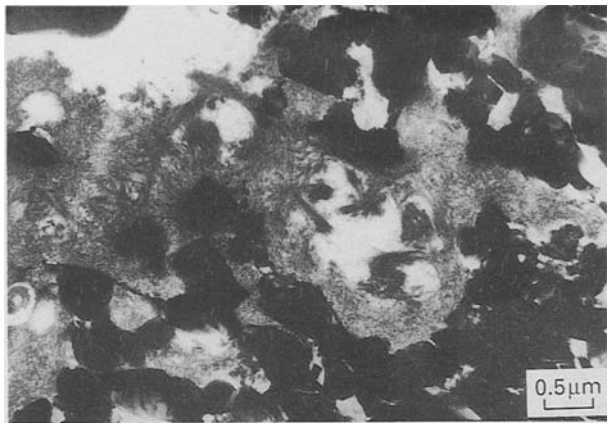

Figure 10 Fibrin-like material covering the implant surface at 3 days after implantation.

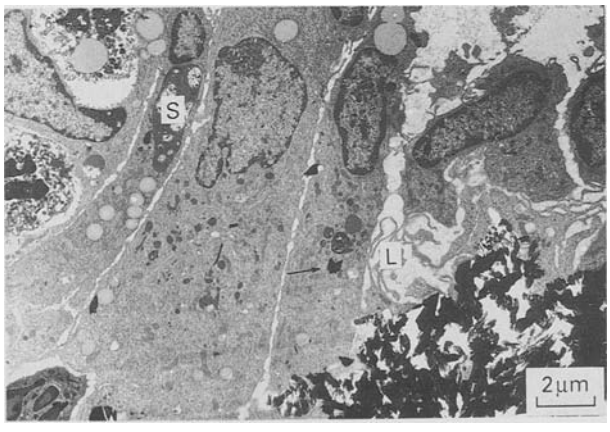

Figure 11 Single layer of macrophage-like cells covering the implant surface at 3 days where the fibrin-like material was not detected. One cell with a secondary lysosome (S), others with lamellopodia (L) or incorporated implant material (arrow).

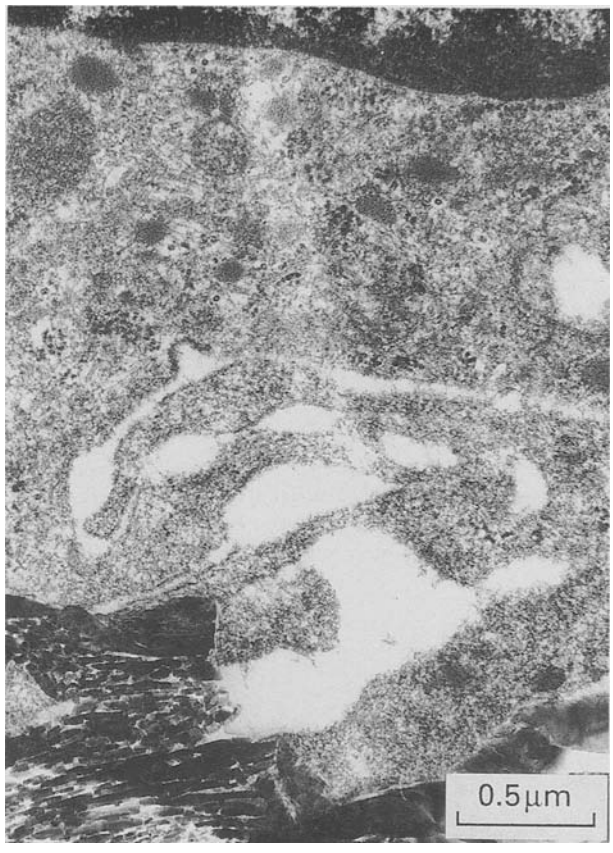

Figure 12 Second crystal moiety of the HA-TCP (lower left) with cellular processes in contact with the implant surface.

cytoplasm, were already found invading the blood clot in some areas. Some collagen fibres were already found in the vicinity of the implant surface. These fibres were not directly attached to the surface.They were separated by cells or cellular processes. In many parts, macrophages were arranged in a single layer on the implant surface. The cells were of about 15 µm in diameter, contained many intracellular lysosomes, and possessed many filopods on their outer cellular membrane (Fig. 11). Some of these cells contained particles of implant origin of about 1–2 µm in diameter within intracellular phagolysosomes. Some of the loose implant particles had not yet been ingested by macrophages, i.e. they were found in the ECM. In some places of the implant surface, a second crystal moiety was detected between the typical HA grains. These particles were much smaller in diameter (0.04 µm on average) (Fig. 12).

At 7 days, many implant surface areas in the TEM-sections were covered with a thin layer of mineralized tissue, which was 0.1–0.5 µm wide. Such mineralization was also observed within macropores of the material and within micropores between grains. The mineralized material within pores did not show the crossbanding of collagen fibres. It appeared rather amorphous in structure and seemed to resemble the intervening layer between mineralized bone and HA as described in former publications [12, 13]. The next layer following this mineralized seam was collagen-rich ECM which contained calcospheritic structures and matrix vesicles. On the ECM osteoblast-like cells were found. Parts of the implant surface, where bonding to bone had not yet occurred, were still covered with a layer of macrophages, only some of which contained particles of implant origin. Between them, single multinuclear giant cells were detected (Fig. 13). In some areas, osteoblast-like cells covered the implant surface followed by ECM and mineralized bone. No evidence was detected to suggest that ECM had been directly produced on the implant surface (Fig. 14). Areas of the drill hole, which were not in contact with the implant surface, consisted of many calcifying areas with collagen-rich ECM, osteoblasts, some capillaries, matrix vesicles, and calcospheritic structures. Some of these calcifying areas produced small calcifying fronts. Fibrin-like material was not detectable. Between HA-TCP particles of a typical size, a second crystal phase was seen in circumscribed areas of the implant surface similar to that described at 3 days after implantation.

At 14 days after implantation, most of the implant surface of the TEM sections, including macropores and micropores, was covered with mineralized tissue. Sometimes osteocytes were found in this layer, totally surrounded by mineralized tissue. In some small areas,

Figure 13 Multinuclear giant cell with extracellular recesses and dorsal ruffling on the implant surface at 3 days after insertion. Note the microcrystalline moiety (arrows) between typical implant grains.

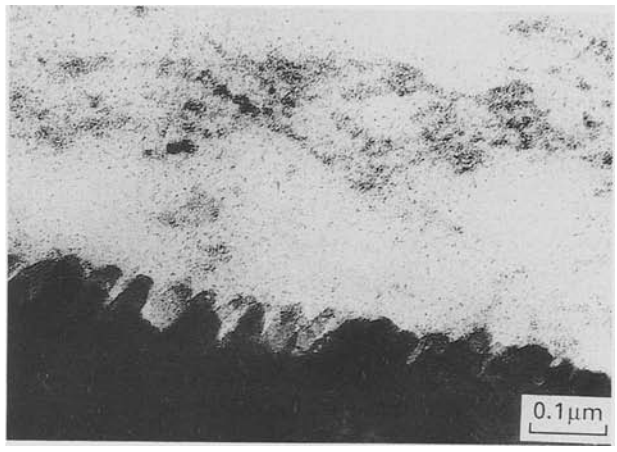

Figure 15 Outer implant surface at 14 days after implantation with grain showing needle-like tips on the implant surface.

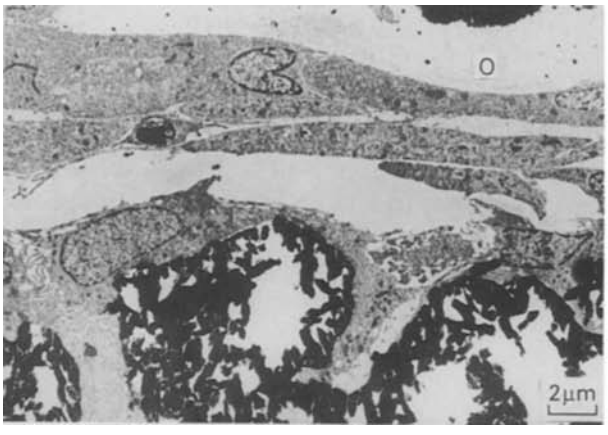

Figure 14 Outer implant surface in a non-bonding area. Single layer of cells in the interface followed by spindle-like cells, osteoid matrix (O), and mineralized bone. Some HA particles were lost during the cutting process.

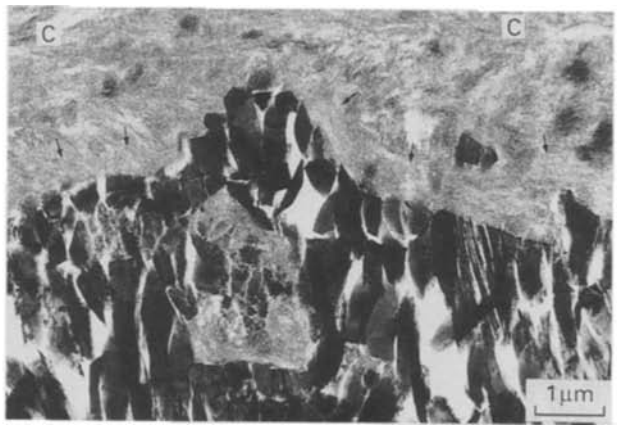

Figure 16 Outer implant surface at 21 days after implantation with HA-TCP grains (black, bottom) and dense mineralization of the interface. Bone bonding via an afibrillar, amorphous-appearing layer (arrows). In some areas of the bone crossbanding of collagen visible (C).

crossbanded fibres, probably collagen, were found in parallel on the HA-TCP surface. These fibres were linked with the implant by a thin amorphous appearing seam. In some sections, bone marrow was observed next to the layer of mineralized tissue in the interface. In these areas of the implant surface, macrophage-like cells were detected in contact with the surface, some of them containing implant particles. Between them, single multinuclear giant cells were observed. A few osteoblasts were found between these macrophages, indicating the phase before mineralization. Some HA-TCP grains in contact with non-mineralized tissue showed tiny tips with diameters of less than 0.05 µm towards the tissue (Fig. 15).

At 21 and 28 days, most of the interface in the TEM-slices was covered with mineralized bone. Sometimes the typical crossbanding of collagen fibres was observed in already mineralized areas, probably due to slight decalcification. Such collagen fibres ran mostly parallel to the implant surface. The mineralized tissue achieved contact with the HA-TCP composite via an afibrillar, amorphous-appearing zone 0.1–0.2 µm wide. Similar material was detected in micropores (Fig. 16). In non-bonding areas of the implant surface, mainly collagen fibres were found parallel to the implant surface. In some areas, cells containing abundant endoplasmic reticulum were detected in direct contact with the HA-TCP surface. Below such cells on the implant grains, an electron dense seam having a mineralized appearance was observed similar to the afibrillar layer of bone bonding zones (Fig. 17). As at 14 days, single macrophages were detectable between osteoblasts. Some particles of implant origin were found in the ECM or ingested by macrophages. Most of the drill hole was filled with dense calcified tissue which formed large calcifying fronts. In between, groups of small capillaries were detected. Some endothelial cells were in contact with the HA-TCP surface. Grains in such areas showed a micro-rugosity which was not observed on grains prior to implantation. No amorphous-appearing afibrillar layer was detectable on the implant surface in such zones (Fig. 18).

4. Discussion

All of the implants were well tolerated and showed intimate contact with bone from the seventh day on.

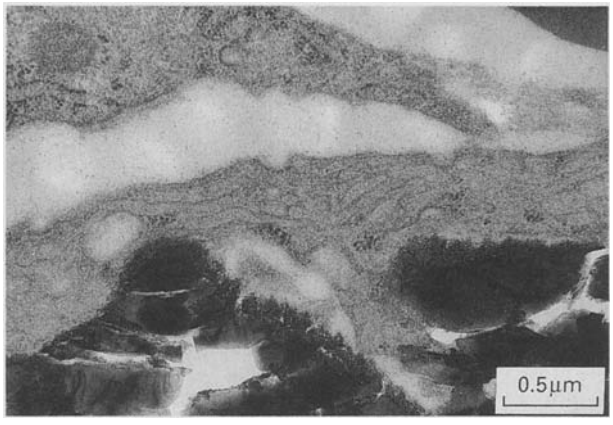

Figure 17 Parts of productive cells, as indicated by high content of smooth endoplasmic reticulum, in contact with the HA-TCP. Between cells and implant surface there is a thin amorphous layer having a mineralized appearance.

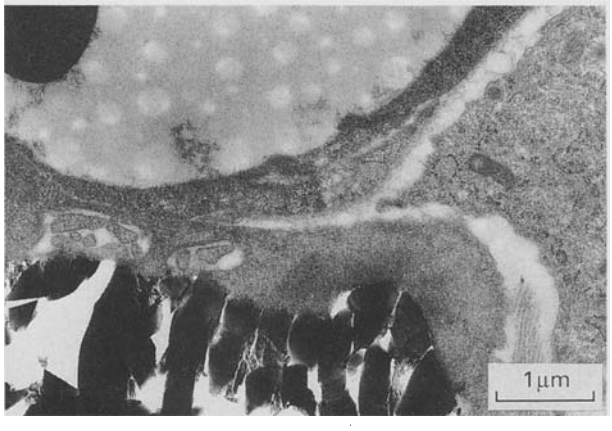

Figure 18 Part of a capillary with an erythrocyte (upper left) close to the HA-TCP surface. Productive cells and extracellular collagen to the right. No afibrillar, amorphous appearing layer on the implant surface. Microroughness of some HA-TCP grains (arrow) pointing to localized degradation.

Implant rectangular blocks were easily separated from the surrounding tissue at 3 days postoperatively. At 7 days and later, however, it became more and more difficult to separate the implant from the tissue, indicating bone-bonding. Sometimes only fragments of the specimens could be obtained due to implants that were broken during fracture between implant and tissue. This suggested that HA-TCP is capable of bonding to bone, which corroborates previous studies [1–7, 12, 20].

One of the important factors which were prerequisites for bone-bonding is the primary mechanical stability of the implant. In other words, micromovement should not exceed a certain value, which is not yet conclusively determined [21]. The micropores and macropores of the HA-TCP porous ceramic surface provided effective anchoring points for various tissue components such as fibres and concomitant mineralization, whereby the implant could be fixed well in the implantation bed. Notably, in the corners and edges of HA porous ceramics, in association with SEM results, the bone-bonding areas appeared obviously earlier and larger than in other parts of the implant surface. It seems that the young bone preferentially bonded with these areas. These areas had initial bone contact immediately after insertion which might account for this reaction. The ingrowth of tissue proceeded from the circumference of the implants towards the centre depending on the time of implantation, which is in accordance with former studies [22–24]. Pore ranges of 70–150 μm in diameter seem to provide a sufficient scaffold for ingrowing bone, which seems to be related to the pore-surface to pore-volume ratio. This finding was corroborated by a former study using biphasic HA with a total porosity of 60% having two different pore diameter ranges (50–100 μm and 200–400 μm, respectively). HA with smaller pores yielded approximately 25% bone within implant pores at 4 months, whereas HA with larger pores developed less than 20% of bone in the implant interstitium at 6 months [23]. Beside the pore diameter, the solubility of the implant material is another important factor determining the rate of bone-bonding. It is well known that implants will be degraded if the solubility is too high; if it is too low the material becomes covered by osteoid and other bone precursor tissues [9]. When compared to other surface reactive materials, such as glass-ceramic KG Cera [25], the lower percentage of bone in the interface of HA implants, measured using histomorphometry, can be related to the lower solubility of the HA implant moiety used here.

The appearance of macrophages on the surface of HA-TCP is especially surprising, since the material is similar to bone HA. Obviously, these cells are able to recognize foreign materials, such as HA-TCP ceramics. This can in part be related to the surface morphology, i.e. to a certain surface roughness or rugosity, and on the other hand to chemical material properties. Their decrease in number seems to be directly correlated to the increase of already mineralized areas of the implant surface which bridge the implant surface microroughness and provide a surface chemistry which is now similar to the mineralized host bone. Such processes seem to start around the third day after implantation (suggested by the SEM results).

The occurrence of macrophages is well in accordance with a former study using glass-ceramics of bone-bonding and non-bonding type. Macrophages disappeared at about 7 days during the onset of mineralization on the bone-bonding implants, whereas they settled on the non-bonding material for at least 14 days [14]. Since many particles of implant origin were found within discrete vacuoles of the macrophage cytoplasm, these cells seem to "clean" the implant surface. A direct resorption of HA bulk implants by macrophages has not yet been observed conclusively. The cells seem to be able to dissolve already ingested bone particles and HA particles [26]. Active resorption of HA implants by osteoclast-like cells *in vivo* was demonstrated in an earlier study [12]. Osteoclast-like cells were observed here in contact with the implants. This might be related to the implant surface morphology with pores and grains, providing a surface rugosity, and to the implant chemistry. The number of osteoclast-like cells on HA-substrata *in vitro* de-

creased with increasing density of the material [27], which points to the importance of implant surface properties in the behaviour of osteoclasts.

The material properties seem to be of utmost importance not only in determining the amount of bone–implant contact but also in determining the rate and mode of implant degradation. Monocrystalline HA was not absorbed *in vitro* [28]. Many studies proved that the material properties of HA, such as macroporosity, microporosity, crystallographic structure, total density, and Ca/P-ratio, are important for the cellular response [29–33].

Some slight changes of the material surface morphology could be detected here at about 7 days, increasing with longer implantation periods. Some single HA-grains changed from a smooth surface to a rough morphology with tiny needle-like crystals, which were obviously not a crystallization on the grain surface. Since these grains were not covered with bone, it seems possible that the changes were induced by leaching of TCP impurities due to soft tissue contact. However, the changes in surface morphology of the HA porous ceramic used here were much less when compared to a former study where pore diameters increased and grain diameters decreased with time [12]. There are several possible explanations available. The crystal size of the present study was higher. Additionally, this might be related to the short implantation period of the present study or to possible impurities of the materials of the former study. Such leaching phenomena led to dissolution, especially in HA intergrain neck regions, and accounted for at least part of the high amount of implant particles in the tissue. This finding is well in accordance with former studies [34–36].

Whether leaching contributed to bone-bonding in promoting the crystallization process, leading to a microscopic layer of apatite on the HA implant surface or whether the mineralized seam on the implant surface is due to active mineralization by cells as suggested by Fig. 17 and former studies [7, 10–13, 16, 17] is not yet clear. Both processes seem to be involved. On the one hand, a fibrin-like organic material was observed on the implant surface and within micropores. Additionally, cells were observed to produce part of the amorphous layer. On the other hand, implant degradation was observed here and the occurrence of a crystallized layer on the implant surface (Fig. 5). Thus, it seems to be likely that reprecipitation processes, depending on the degradability of the material, participate in bone-bonding. All these different processes i.e. mineralization by cells, epitaxy, dissolution and reprecipitation, indicate a mechanism of centrifugal mineralization, i.e. a process starting on the implant surface and proceeding into the tissue surrounding the implant. This interpretation would explain the amorphous intervening interface layer observed here and in former studies [12, 13, 37]. In the case of HA ceramics, distinct bonding zones were observed without the above described intervening layer [12, see Fig. 5]. Such zones seem to be produced by different processes, i.e. the perpendicular or oblique insertion of collagen and subsequent mineralization. On the other hand, an amorphous interface layer seems to be produced when the crystallization of amorphous material preceeds the insertion of collagen. Mineralized layers at HA bone interfaces contained carbonated apatitic crystals which were similar to the surrounding bone mineral [38, 39]. The formation of such layers is a typical feature of HA implants in aqueous solutions, since similar layers also develop in non-osseous implantation sites [40].

In conclusion, HA porous ceramics were well incorporated in bone by bone-bonding and seem to be suitable for non-loaded or partially loaded applications. Pores in the range 70–150 μm provide a sufficient scaffold for bone ingrowth. Amorphous intervening layers were observed, probably being produced by active secretion of cells and/or by epitaxy providing a connection between mineralized bone, i.e. mineralized collagen, and HA-TCP implants. Zones without such a layer seem to be related to early collagen insertion and subsequent mineralization.

Acknowledgements

This study was supported by the Deutsche Forschungsgemeinschaft, Bonn, FRG. The material was produced in the laboratory of the Institute of Material Science, Sichuan University, Peoples Republic of China. For typing the manuscript the authors thank Dr Susanne Müller-Mai.

References

1. A. S. POSNER, F. BETTS and N. C. BLUMENTHAL, *Prog. Crystal Growth Charact.* **3** (1980) 49.
2. U. M. GROSS, C. MÜLLER-MAI and C. VOIGT, *Biomaterials* **11** (1990) 83.
3. H. W. DENISSEN, K. DE GROOT, P. C. MAKKES, A. VAN DEN HOOFF and P. J. KLOPPER, *J. Biomed. Mater. Res.* **14** (1980) 713.
4. H. W. DENISSEN, A. A. H. VELDHUIS, H. W. B. JANSEN and A. VAN DEN HOOFF, *ibid.* **18** (1984) 147.
5. R. E. HOLMES, *Plastic and Reconstructive Surg.* **63** (1979) 626.
6. R. E. HOLMES, R. W. BUCHHOLZ and V. MOONEY, *J. Bone Joint Surg.* **68-A** (1986) 904.
7. M. JARCHO, *Clin. Orthop. Rel. Res.* **157** (1981) 259.
8. L. L. HENCH, R. J. SPLINTER, W. C. ALLEN and T. K. GREENLEE, *J. Biomed. Mater. Res. Symp.* **2** (1971) 117.
9. U. GROSS and V. STRUNZ, *J. Biomed. Mater. Res.* **19** (1985) 251.
10. M. NEO, S. KOTANI, T. NAKAMURA, T. YAMAMURO, Y. BANDO, C. OHTSUKE and T. KOKUBO, *ibid.* **26** (1992) 1419.
11. C. M. MÜLLER-MAI, C. VOIGT, R. E. BAIER and U. M. GROSS, *Cells and Materials* **2** (1992) 309.
12. C. M. MÜLLER-MAI, C. VOIGT and U. M. GROSS, *Scanning Microsc.* **4** (1990) 613.
13. M. NEO, S. KOTANI, T. NAKAMURA, T. YAMAMURO, C. OHTSUKI, T. KOKUBO and Y. BANDO, *J. Biomed. Mater. Res.* **26** (1992) 255.
14. C. MÜLLER-MAI, C. VOIGT, W. KNARSE, J. SELA and U. M. GROSS, *Biomaterials* **12** (1991) 865.
15. L. L. HENCH and G. LATORRE, in "Bioceramics", Vol. 5, edited by T. Yamamuro, T. Kokubo and T. Nakamura (Kobunshi Kankokai, Kyoto, Japan, 1992) p. 67.
16. J. E. DAVIES, R. CHERNECKY, B. LOWENBERG and A. SHIGA, *Cells and Materials* **1** (1991) 3.
17. B. LOWENBERG, R. CHERNECKY, A. SHIGA and J. E. DAVIES, *ibid.* **1** (1991) 177.

18. X. ZHANG, Z. JIMING, W. CHEN, C. WU and P. ZHOU, Transactions, 4th World Biomaterials Congress, Berlin, 1992, p. 332.
19. U. M. GROSS and V. STRUNZ, *Stain Technol.* **52** (1977) 217.
20. M. JARCHO, J. F. KAY, K. J. GUMAER, R. H. DOREMUS and H. P. DROBECK, *J. Bioeng.* **1** (1977) 79.
21. R. M. PILLIAR, J. M. LEE and C. MANIATOPOULOS, *Clin. Orthop. Rel. Res.* **208** (1986) 108.
22. G. DACULSI, N. PASSUTI, S. MARTIN, C. DEUDON, R. Z. LEGEROS and S. RAHER, *J. Biomed. Mat. Res.* **24** (1990) 379.
23. P. S. EGGLI, W. MÜLLER and R. K. SCHENK, *Clin. Orthop. Rel. Res.* **232** (1988) 127.
24. S. D. COOK, K. A. THOMAS, J. F. KAY and M. JARCHO, *ibid.* **230** (1988) 303.
25. C. M. MÜLLER-MAI, C. VOIGT, R. E. BAIER and U. GROSS, Transactions, 4th World Biomaterials Congress, April 24-28, 1992, Berlin, p. 237.
26. C. H. KWONG, W. B. BURNS and H. S. CHEUNG, *Biomaterials* **10** (1989) 579.
27. M. OGURA, T. SAKAE and J. E. DAVIES, in "Bioceramics", Vol. 4, edited by W. Bonfield and G. W. Hastings (Butterworth-Heinemann, Oxford, 1991) p. 121.
28. H. SHIMIZU, S. SAKAMOTO, M. SAKAMOTO and D. D. LEE, *Bone and Mineral* **6** (1989) 261.
29. K. DE GROOT, *Biomaterials* **1** (1980) 47.
30. K. KÖSTER, E. KARBE, H. KRAMER, H. HEIDE and R. KÖNIG, *Langenbecks Arch. Chir.* **341** (1976) 77.
31. C. P. A. T. KLEIN, A. A. DRIESSENS, K. DE GROOT and A. VAN DEN HOOFF, *J. Biomed. Mater. Res.* **17** (1983) 769.
32. C. P. A. T. KLEIN, K. DE GROOT, A. A. DRIESSENS and H. B. M. VAN DER LUBBE, *Biomaterials* **6** (1985) 189.
33. *Idem., ibid.* **7** (1986) 144.
34. J. BECKER, A. KUNTZ, U. GROSS, F. E. FENSCH, W. KÜPPER and P. REICHART, Z. ZAHNÄRZTL, *Implantol.* **3** (1987) 200.
35. C. A. VAN BLITTERSWIJK, W. KUIPERS, W. T. DAEMS and K. DE GROOT, *Biomaterials* **7** (1986) 137.
36. M. WINTER, P. GRISS, K. DE GROOT, H. TAGAI, G. HEIMKE, H. J. A. VAN DIJK and K. SAWAI, *ibid.* **2** (1981) 159.
37. J. D. DE BRUIJN, J. E. DAVIES, C. P. A. T. KLEIN, K. DE GROOT, C. A. VAN BLITTERSWIJK, in "Bone-binding biomaterials" (Reed Healthcare Communications, Liediendorp, NL, 1992) p. 57.
38. I. ORLY, M. GREGOIRE, J. MENANTEAU, M. HEUGHEBAERT and B. KEREBEL, *Calcif. Tissue Int.* **45** (1989) 20.
39. G. DACULSI, R. Z. LEGEROS, M. HEUGHEBAERT and I. BARBIEUX, *ibid.* **46** (1990) 20.
40. M. HEUGHEBAERT, R. Z. LEGEROS, M. GINESTE, A. GUILHEM and G. BONEL, *J. Biomed. Mater. Res.* **22** (1988) 257.

Received 17 July 1993
and accepted 16 January 1994